Aerospace Systems (2018) 1:129–137
https://doi.org/10.1007/s42401-018-0013-0

ORIGINAL PAPER

# Modal equivalent method of full-area membrane and grid membrane

Yibei Zhang[1] · Wujun Chen[1] · Chao Xie[2] · Fujun Peng[2]

Received: 22 July 2018 / Revised: 5 November 2018 / Accepted: 13 November 2018 / Published online: 10 December 2018


## Abstract

Pre-tension rectangular membrane is a promising structure in space engineering due to lightweight, high area-to-weight ratio and excellent folding capability. However, its dynamic characteristic of ground experiment can be largely affected by air, meaning the vibration behavior in air is quite different from the behavior in orbit vacuum. Therefore, a grid membrane is explored as the alternative structure, which can be less affected by air. Based on the small deformation theory, a modal equivalent method is established to make the natural frequencies and vibration modes of the original full-area membrane and the alternative grid membrane identical. A finite element code is utilized to verify this method, and the modals of the two structures are basically same. Meanwhile, a fluid–structure coupling simulation is conducted. The result indicates that the air effect on the alternative grid membrane is quite small compared with the original full-area membrane. Consequently, this grid membrane can be used as the alternative structure of the full-area membrane, as a mean to reduce the air effects in a ground structure experiment.

**Keywords** Pre-tension rectangular membrane · Grid membrane · Modal equivalent method · Air effect

## 1 Introduction

Pre-tension rectangular membrane is a promising structure in space engineering due to lightweight, high area-to-weight ratio and excellent folding capability. However, it is difficult to conduct a ground structure vibration experiment of a spacecraft with this kind of structure as a component, because the dynamic characteristic of the membrane can be largely affected by air, meaning that the vibration behavior in air is quite different from the behavior in vacuum [1–4]. Consequently, when conducting a ground experiment to study the natural frequency of a membrane, the air effect should be reduced.

Generally, there are two ways to reduce this air effect: the first one is conducting the vibration experiment in a vacuum device. The vacuum environment in the device is nearly the same as the environment in aerospace. Therefore, this method is the most direct way to proceed with a ground experiment to simulate the vibration of a membrane in aerospace. However, the size of the vacuum device cannot be large and the cost is quite expensive. Therefore, this method can only conduct a reduced-scale experiment. The second one is using an alternative structure to substitute the membrane and this structure should be less sensitive to air. Moreover, these two structures should have the same natural frequencies and vibration modes. For the convenience of expression, the original structure is called full-area membrane. In this paper, a grid membrane is explored as the alternative structure, which is consisted of crossed membrane strips in longitude and latitude directions. The space between the strips can guarantee a free airflow, meaning that this structure can be less affected by air.

The equivalent criterion of the full-area membrane and grid membrane should be established. In recent years, several equivalent criteria considering different kinds of structures have been proposed. Liu [5] considered a hoop truss structure as a beam model, and used an energy equivalence method to establish the equivalent criterion. Xu [6] deemed a membrane SAR (Synthetic Aperture Radar) as a cantilever beam and utilized the Vector Form Intrinsic Finite Element (VFIFE) method to establish the equivalent model. There are more researchers used the beam theory to study an inflated fabric tube [7, 8]. In their studies, the original structure is usually complex and there may not exist a standard theory for

✉ Wujun Chen
cwj@sjtu.edu.cn

1 Shanghai Jiao Tong University Space Structure Research Center, Shanghai 200240, China

2 Aerospace System Engineering Shanghai, Shanghai 201108, China

analysis. By simplifying the original structure into the substituting structure, one can establish the equivalent method, meaning that the original structure may not have to be well studied. However, the substituting structure must be analyzed in detail. In this paper, the original structure (full-area membrane) is quite simple compared with the substituting structure (grid membrane). Therefore, both the two models need to be well studied.

This paper proposes a modal equivalent method to make the full-area membrane and the grid membrane the same natural frequencies and vibration modes, based on the small deformation theory. The second section gives a detailed illustration of modal equivalent method. The third section uses a Finite Element (FE) code to verify this modal equivalent method. The natural frequencies and vibration modes of the two structures are nearly same. Therefore, the modal equivalent method proposed by this paper is valid.

## 2 Modal equivalent method

When using a grid membrane to substitute the full-area membrane, the modal equivalent method should be established. This paper focuses on the small deformation theory. The stress field of the structure is assumed as homogeneous and constant, meaning that the stress field is not a function of $x$ and $y$ ($x$ and $y$ represent the coordinates).

The main content of the equivalent theory is as follows: firstly, the dynamic equilibrium equation of an infinitesimal element should be established. Secondly, based on the Galerkin method, the dynamic equations of the grid membrane and full-area membrane can be built. Finally, by comparing the coefficients in the dynamic equations of the two different structures, the modal equivalent criterion can be obtained.

### 2.1 Dynamic equation of an infinitesimal element

The infinitesimal element under tensile forces and shear forces is shown in Fig. 1. The parameters shown in Fig. 1 are all defined based on the global coordinate system. When the normal stresses of the membrane are considerably large, the bending moment can be neglected as its value is relatively small. While the bending moment must be considered in a wrinkle analysis, since one of the normal stress will be quite small [9]. The resultant force of the internal forces in the deflection direction is as follows:

$$\begin{aligned} F_{z\_\mathrm{inner}} = & \frac{\partial N_x}{\partial x}\sin\theta \mathrm{d}x\mathrm{d}y + N_x\frac{\partial\theta}{\partial x}\cos\theta \mathrm{d}x\mathrm{d}y \\ & + \frac{\partial N_y}{\partial y}\sin\varphi \mathrm{d}x\mathrm{d}y + N_y\frac{\partial\varphi}{\partial y}\cos\varphi \mathrm{d}x\mathrm{d}y \\ & + \frac{\partial N_{yx}}{\partial y}\sin\theta \mathrm{d}x\mathrm{d}y + N_{yx}\frac{\partial\theta}{\partial y}\cos\theta \mathrm{d}x\mathrm{d}y \\ & + \frac{\partial N_{xy}}{\partial x}\sin\varphi \mathrm{d}x\mathrm{d}y + N_{xy}\frac{\partial\varphi}{\partial x}\cos\varphi \mathrm{d}x\mathrm{d}y \end{aligned} \tag{1}$$

where $N_x$ and $N_y$ denote the tensile forces in unit length; $N_{yx}$ and $N_{xy}$ denote the shear forces in unit length; $\theta$ is the angle between $N_x$ and $x$-axis; and $\varphi$ is the angle between $N_y$ and $y$-axis.

The inertia force in the deflection direction is considered as the external force. Based on the above hypothesis, its expression is written as follows:

$$F_{z\_\mathrm{inertia}} = \rho h\left(\frac{\mathrm{d}x\mathrm{d}y}{\cos\theta\cos\varphi}\right)\frac{\partial^2 z}{\partial t^2} \tag{2}$$

where $\rho$ is the density of the membrane and $h$ is the thickness of the membrane.

According to the D'Alembert's principle, and combining Eqs. (1) and (2), the dynamic equation that considers tensile forces, shear forces and inertia force is written as follows:

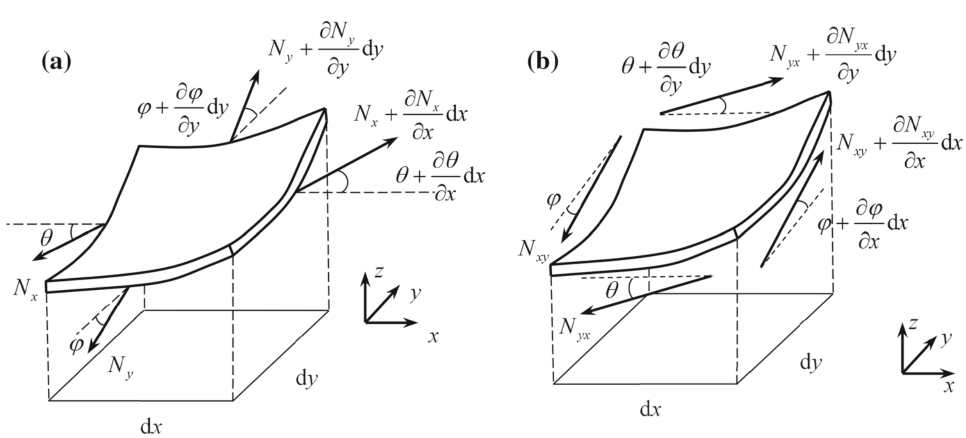


**Fig. 1** The microelement with inner forces: **a** Tensile forces; **b** Shear forces

$$\frac{\partial^2 z}{\partial t^2} = \frac{\cos\theta\cos\varphi}{\rho h}\left[\left(N_x\frac{\partial\theta}{\partial x} + N_{yx}\frac{\partial\theta}{\partial y}\right)\cos\theta + \left(N_y\frac{\partial\varphi}{\partial y} + N_{xy}\frac{\partial\varphi}{\partial x}\right)\cos\varphi + \left(\frac{\partial N_x}{\partial x} + \frac{\partial N_{yx}}{\partial y}\right)\sin\theta + \left(\frac{\partial N_y}{\partial y} + \frac{\partial N_{xy}}{\partial x}\right)\sin\varphi\right] \tag{3}$$

Then, consider some geometry relationships as follows:

$$\tan\theta = \frac{\partial z}{\partial x},\ \tan\varphi = \frac{\partial z}{\partial y}$$

Differentiating both sides of the above equations by $x$ or $y$ [10], one can yield that

$$\frac{\partial\theta}{\partial x} = cos^2\theta\frac{\partial^2 z}{\partial x^2},\ \frac{\partial\theta}{\partial y} = cos^2\theta\frac{\partial^2 z}{\partial x\partial y}$$

$$\frac{\partial\varphi}{\partial x} = cos^2\varphi\frac{\partial^2 z}{\partial x\partial y},\ \frac{\partial\varphi}{\partial y} = cos^2\varphi\frac{\partial^2 z}{\partial y^2}$$

When the vibration deformation is small, $\theta$ and $\varphi$ can be deemed as zero. Therefore

$$\sin\theta = 0,\ \cos\theta = 1,\ \sin\varphi = 0,\ \cos\varphi = 1$$

Moreover, when the deformation is small, the stress field of the membrane can be treated as constant and equals to the pre-stress state. Usually, the predominant item in the pre-stressed field is normal stress and the shear stress is relatively small and negligible. Then, one can yield that

$$N_x = N_{x0},\ N_y = N_{y0},\ N_{xy} = N_{yx} = 0$$

Consequently, based on the small deformation theory, the dynamic equation of the infinitesimal element can be transformed as follows:

$$\frac{\partial^2 z}{\partial t^2} = \frac{1}{\rho h}\left(N_{x0}\frac{\partial^2 z}{\partial x^2} + N_{y0}\frac{\partial^2 z}{\partial y^2}\right)$$

The separation variable method and the modal superposition method are utilized to solve the above partial differential equation. The deflection parameter $z$ can be assumed as follows:

$$z(x, y, t) = \left[\sum_{m,n} Z_{mn}(x, y)\right] T_{mn}(t)$$

where $Z_{mn}(x,y)$ represents the $(m,n)$th vibration mode; $T_{mn}(t)$ represents the $(m,n)$th time-history vibration component. According to the Galerkin method, and considering the orthogonality between two different modes, the dynamic equation of the $(m,n)$th modal can be transformed as follows:

$$\oiint_S \left[Z_{mn}\frac{\mathrm{d}^2 T_{mn}}{\mathrm{d}t^2} - \frac{1}{\rho h}\left(N_{x0}\frac{\partial^2 Z_{mn}}{\partial x^2} + N_{y0}\frac{\partial^2 Z_{mn}}{\partial y^2}\right)T_{mn}\right]Z_{mn}\,\mathrm{d}S = 0 \tag{4}$$

where $S$ represents the integral region of the membrane. Equation (4) can be simply written as follows:

$$\frac{\mathrm{d}^2 T_{mn}}{\mathrm{d}t^2} + \omega_{mn}^2 T_{mn} = 0 \tag{5}$$

where

$$A_{mn} = \oiint_S Z_{mn}^2\,\mathrm{d}S \tag{6}$$

$$\omega_{mn}^2 = -\frac{1}{\rho h A_{mn}}\oiint_S \left(N_{x0}\frac{\partial^2 Z_{mn}}{\partial x^2} + N_{y0}\frac{\partial^2 Z_{mn}}{\partial y^2}\right)Z_{mn}\,\mathrm{d}S \tag{7}$$

From the dynamic equation above, one can get that $\omega_{mn}$ is the natural frequency.

## 2.2 Frequency of full-area membrane

The original full-area membrane is shown in Fig. 2. The length of the membrane is $a_1$; the width is $b_1$; the thickness is $h_1$; the density is $\rho_1$. The subscript '1' represents the parameters of the original full-area membrane.

The four edges of the membrane are simply supported. Therefore, the $(m,n)$th vibration mode can be assumed as follows:

$$Z_{mn\_1}(x, y) = \sin\left(\frac{m\pi x}{a_1}\right)\sin\left(\frac{n\pi y}{b_1}\right) \tag{8}$$

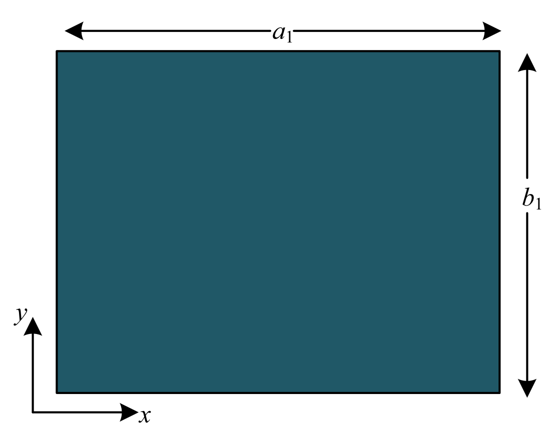


**Fig. 2** Full-area membrane

Substituting Eq. (8) into Eqs. (6) and (7), one can get that

$$A_{mn\_1} = \iint_S Z_{mn\_1}^2 \mathrm{d}S = \frac{a_1 b_1}{4} \tag{9}$$

$$\omega_{mn\_1}^2 = \frac{1}{\rho_1 h_1}\left[N_{x0\_1}\left(\frac{m\pi}{a_1}\right)^2 + N_{y0\_1}\left(\frac{n\pi}{b_1}\right)^2\right] \tag{10}$$

## 2.3 Frequency of grid membrane

The alternative grid membrane is shown as Fig. 3. The length of the grid membrane is $a_2$; the width is $b_2$; the thickness is $h_2$; the density is $\rho_2$; the width of the $x$-direction strip is $d_{x\_2}$; the width of the $y$-direction strip is $d_{y\_2}$. The strips are uniformly distributed. The number of the $x$-direction strip is $n_{x\_2}$; the number of the $y$-direction strip is $n_{y\_2}$. The subscript '2' represents the parameters of the alternative grid membrane.

The global geometry of the alternative grid membrane should be identical to the original full-area membrane. Therefore

$$a_1 = a_2, \;\; b_1 = b_2$$

The edges of the grid membrane are also simply supported. The $(m,n)$th vibration mode can still be assumed as follows:

$$Z_{mn\_2}(x, y) = \sin\left(\frac{m\pi x}{a_2}\right)\sin\left(\frac{n\pi y}{b_2}\right) \tag{11}$$

Substituting Eq. (11) into Eqs. (6) and (7), one can yield that

$$\begin{aligned} A_{mn\_2} &= \iint_{S_{x\_2}} Z_{mn\_2}^2 \mathrm{d}S + \iint_{S_{y\_2}} Z_{mn\_2}^2 \mathrm{d}S \\ &= \sum_{i=1}^{n_{x\_2}}\left[\int_0^{a_2}\sin^2\left(\frac{m\pi x}{a_2}\right)\mathrm{d}x \int_{y_{i\_2\_1}}^{y_{i\_2\_2}}\sin^2\left(\frac{n\pi y}{b_2}\right)\mathrm{d}y\right] \\ &\quad + \sum_{i=1}^{n_{y\_2}}\left[\int_{x_{i\_2\_1}}^{x_{i\_2\_2}}\sin^2\left(\frac{m\pi x}{a_2}\right)\mathrm{d}x \int_0^{b_2}\sin^2\left(\frac{n\pi y}{b_2}\right)\mathrm{d}y\right] \\ &= \frac{a_2}{2}\sum_{i=1}^{n_{x\_2}}\int_{y_{i\_2\_1}}^{y_{i\_2\_2}}\sin^2\left(\frac{n\pi y}{b_2}\right)\mathrm{d}y \\ &\quad + \frac{b_2}{2}\sum_{i=1}^{n_{y\_2}}\int_{x_{i\_2\_1}}^{x_{i\_2\_2}}\sin^2\left(\frac{m\pi x}{a_2}\right)\mathrm{d}x \end{aligned} \tag{12}$$

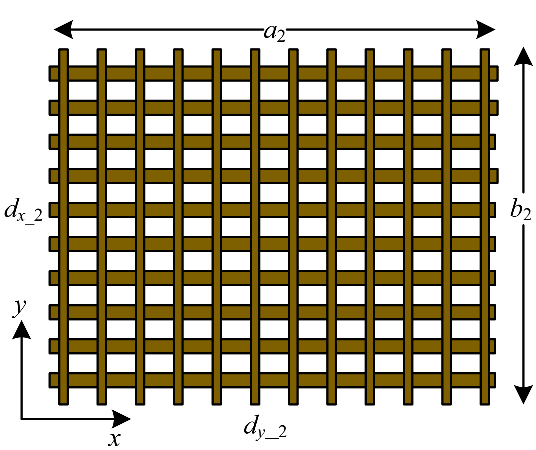


Fig. 3 Grid membrane

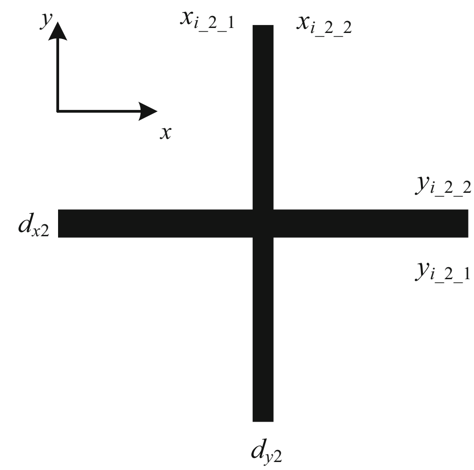


Fig. 4 Diagram of an $x$-direction strip and a $y$-direction strip

$$\begin{aligned} \omega_{mn\_2}^2 &= -\frac{N_{x0\_2}}{\rho_2 h_2 A_{mn\_2}}\iint_{S_{x\_2}}\frac{\partial^2 Z_{mn}}{\partial x^2}Z_{mn}\mathrm{d}S \\ &\quad - \frac{N_{y0\_2}}{\rho_2 h_2 A_{mn\_2}}\iint_{S_{y\_2}}\frac{\partial^2 Z_{mn}}{\partial y^2}Z_{mn}\mathrm{d}S \\ &= \frac{1}{\rho_2 h_2 A_{mn\_2}}\left[\frac{a_2 N_{x0\_2}}{2}\left(\frac{m\pi}{a_2}\right)^2\sum_{i=1}^{n_{x\_2}}\int_{y_{i\_2\_1}}^{y_{i\_2\_2}}\sin^2\left(\frac{n\pi y}{b_2}\right)\mathrm{d}y\right. \\ &\quad \left. + \frac{b_2 N_{y0\_2}}{2}\left(\frac{n\pi}{b_2}\right)^2\sum_{i=1}^{n_{y\_2}}\int_{x_{i\_2\_1}}^{x_{i\_2\_2}}\sin^2\left(\frac{m\pi x}{a_2}\right)\mathrm{d}x\right] \end{aligned} \tag{13}$$

where $S_{x\_2}$ represents the integral region of the $x$-direction strips. $S_{y\_2}$ represents the integral region of the $y$-direction strips. $x_{i\_2\_1}$ and $x_{i\_2\_2}$ are the $x$-coordinates of the two lateral sides of the $i$th $y$-direction strip. $y_{i\_2\_1}$ and $y_{i\_2\_2}$ are the $x$-coordinates of the two lateral sides of the $i$th $y$-direction strip. The diagram of an $x$-direction strip and a $y$-direction strip is shown in Fig. 4.

As the strips are uniformly distributed, the lateral side coordinates of the strips can be expressed as follows:

$$x_{i\_2\_1} = \left(\frac{i}{n_{y\_2}} - \frac{1}{2n_{y\_2}}\right)a_2 - \frac{d_{y\_2}}{2},$$
$$x_{i\_2\_2} = \left(\frac{i}{n_{y\_2}} - \frac{1}{2n_{y\_2}}\right)a_2 + \frac{d_{y\_2}}{2}$$

**Table 1** Material properties of the structures

| | $h$ (m) | $\rho$ (kg/m$^3$) | $Ex$ (GPa) | $Ey$ (GPa) | $G$ (GPa) | $\mu$ |
|---|---|---|---|---|---|---|
| Full-area | 0.0001 | 1600 | 4 | 6 | 2 | 0.3 |
| Grid | 0.0002 | 1300 | 2 | 2 | 0.74 | 0.35 |

$$y_{i\_2\_1} = \left(\frac{i}{n_{x\_2}} - \frac{1}{2n_{x\_2}}\right)b_2 - \frac{d_{x\_2}}{2},$$
$$y_{i\_2\_2} = \left(\frac{i}{n_{x\_2}} - \frac{1}{2n_{x\_2}}\right)b_2 + \frac{d_{x\_2}}{2}$$

Therefore

$$x_{i\_2\_1} + x_{i\_2\_2} = \left(\frac{2i}{n_{y\_2}} - \frac{1}{n_{y\_2}}\right)a_2,\ x_{i\_2\_2} - x_{i\_2\_1} = d_{y\_2}$$

$$y_{i\_2\_1} + y_{i\_2\_2} = \left(\frac{2i}{n_{x\_2}} - \frac{1}{n_{x\_2}}\right)b_2,\ y_{i\_2\_2} - y_{i\_2\_1} = d_{x\_2}$$

Equation (12) and Eq. (13) can be further simplified as follows, and the specific process is shown in the Appendix A.

$$A_{mn\_2}=\frac{a_2 n_{x\_2}}{4}d_{x\_2} + \frac{b_2 n_{y\_2}}{4}d_{y\_2}$$

$$\omega^2_{mn\_2} = \frac{1}{\rho_2 h_2 A_{mn\_2}}\left[N_{x0\_2}\left(\frac{m\pi}{a_2}\right)^2 \frac{a_2 n_{x\_2}}{4}d_{x\_2} + N_{y0\_2}\left(\frac{n\pi}{b_2}\right)^2 \frac{b_2 n_{y\_2}}{4}d_{y\_2}\right]$$

When $a_2 n_{x\_2} d_{x\_2} = b_2 n_{y\_2}$, one can yield that

$$A_{mn\_2} = \frac{a_2 n_{x\_2}}{4}d_{x\_2} + \frac{b_2 n_{y\_2}}{4}d_{y\_2} = \frac{a_2 n_{x\_2}}{2}d_{x\_2} = \frac{b_2 n_{y\_2}}{2}d_{y\_2}$$

$$\omega^2_{mn\_2} = \frac{1}{\rho_2 h_2}\left[N_{x0\_2}\left(\frac{m\pi}{a_2}\right)^2 + N_{y0\_2}\left(\frac{n\pi}{b_2}\right)^2\right]\frac{a_2 n_{x\_2}}{4A_{mn\_2}}d_{x\_2} = \frac{1}{2\rho_2 h_2}\left[N_{x0\_2}\left(\frac{m\pi}{a_2}\right)^2 + N_{y0\_2}\left(\frac{n\pi}{b_2}\right)^2\right] \quad (14)$$

### 2.4 Modal equivalent criterion

Comparing Eqs. (10) and (14), which are the frequency expressions of the original full-area membrane and the alternative grid membrane, one can yield the equivalent criterion as follows:

$$\frac{N_{x0\_2}}{\rho_2 h_2} = 2\frac{N_{x0\_1}}{\rho_1 h_1},\ \frac{N_{y0\_2}}{\rho_2 h_2} = 2\frac{N_{y0\_1}}{\rho_1 h_1}$$

Meanwhile, the following requirements must be satisfied:

(1) The strips must be uniformly distributed;
(2) $a_2 n_{x\_2} d_{x\_2} = b_2 n_{y\_2} d_{y\_2}$;
(3) $\frac{n}{n_{x\_2}} \notin \mathbf{Z}$ and $\frac{m}{n_{y\_2}} \notin \mathbf{Z}$.

## 3 Simulation and theory verification

WORKBENCH is utilized as the FE code to verify the above modal equivalent method. The geometry and material properties of the original full-area membrane and the alternative grid membrane are shown in Table 1.

The length of the structures is $a_1 = a_2 = 1$ m and the width is $b_1 = b_2 = 0.8$ m. The strips of the grid membrane are uniformly distributed. In order to make the first five modals of the two structures equivalent, the number of the $x$-direction strip is set as $n_{x\_2} = 3$, and the number of the $y$-direction strip is set as $n_{y\_2} = 7$. The width of the $x$-direction strip is set as $d_{x\_2} = 0.02$ m. Therefore, according to the equivalent criterion, the width of the $y$-direction strip should be

$$d_{y\_2} = \frac{a_2 n_{x\_2}}{b_2 n_{y\_2}}d_{x\_2} = 0.0108\,\text{m}$$

The initial tensile forces in unit length of the full-area membrane are set as $N_{x0\_1} = 200$ N/m and $N_{y0\_1} = 300$ N/m. According to the equivalent criterion, the initial tensile forces in unit length of the grid membrane are set as follows:

$$N_{x0\_2} = \frac{2\rho_2 h_2}{\rho_1 h_1}N_{x0\_1} = 650\,\text{N/m}$$

$$N_{y0\_2} = \frac{2\rho_2 h_2}{\rho_1 h_1}N_{y0\_1} = 975\,\text{N/m}$$

Therefore, the initial pre-tension of the two structures can be calculated as follows:

$$F_{x0\_1} = N_{x0\_1}b_1 = 160\text{N},\ F_{y0\_1} = N_{y0\_1}a_1 = 300\,\text{N}$$
$$F_{x0\_2} = N_{x0\_2}d_{x\_2}n_{x\_2} = 39\text{N},$$
$$F_{y0\_2} = N_{y0\_2}d_{y\_2}n_{y\_2} = 73.71\,\text{N}$$

In the simulation, the force and displacement boundary conditions of the two structures are set as Figs. 5 and 6.

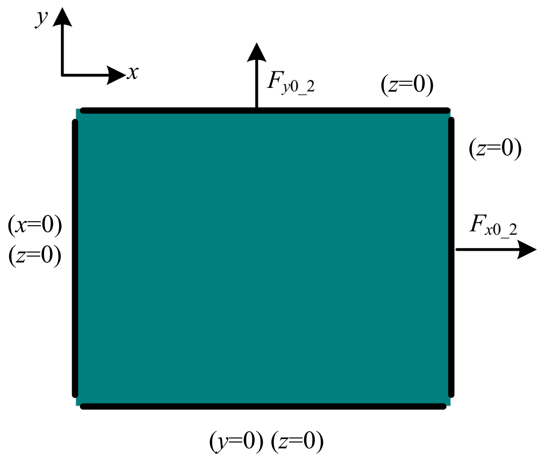


**Fig. 5** Boundary conditions of the full-area membrane

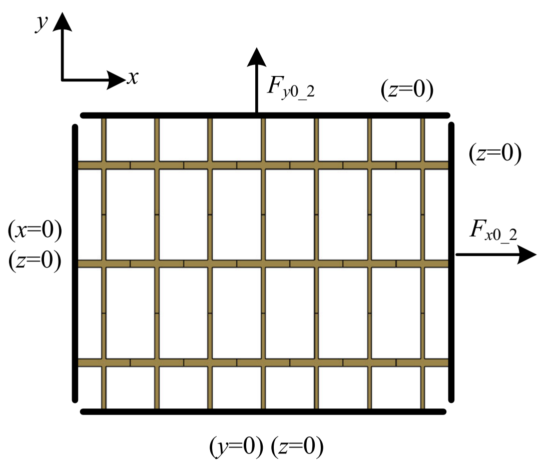


**Fig. 6** Boundary conditions of the grid membrane

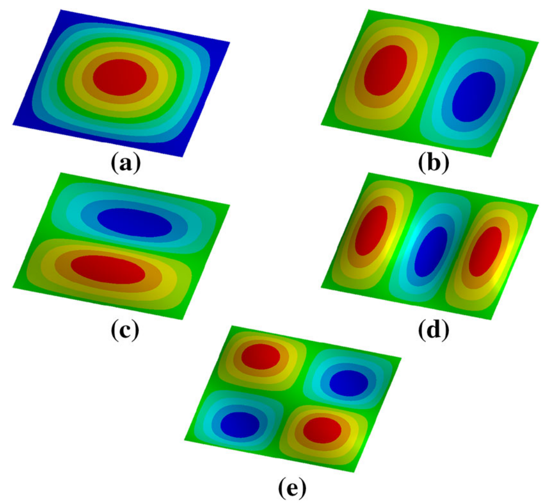


**Fig. 7** The first five vibration modes of the full-area membrane. **a** 1st mode; **b** 2nd mode; **c** 3rd mode; **d** 4th mode; **e** 5th mode

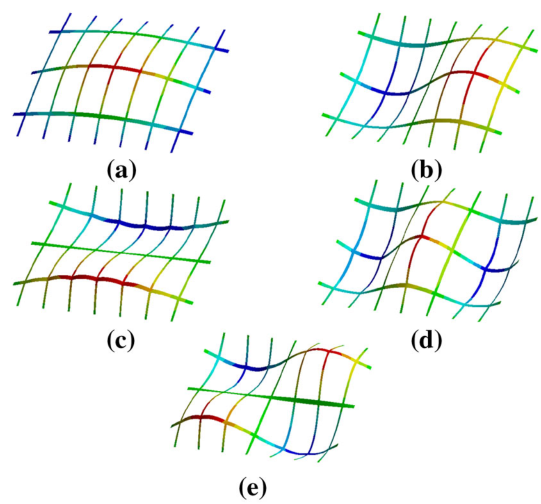


**Fig. 8** The first five modes of the grid membrane. **a** 1st mode; **b** 2nd mode; **c** 3rd mode; **d** 4th mode; **e** 5th mode

## 3.1 Vacuum circumstance

In this example, the air effect is not considered, and the natural frequencies and vibration modes are obtained based on the eigenvalue decomposition method. The first five vibration modes of the full-area membrane are shown in Fig. 7, and the first five vibration modes of the grid membrane are shown in Fig. 8. The related frequencies are shown in Table 2. The frequencies of the original full-area membrane are basically equal to the alternative grid membrane, and the relative deviations are quite small. Moreover, the vibration modes are basically same.

## 3.2 Air circumstance

The natural frequency considering air effect cannot be calculated by the eigenvalue decomposition method directly. However, it can be obtained from the time-history vibration data. Based on the Transient Structural module and the CFX module in WORKBENCH, the Fluid Solid Interaction (FSI) analysis is utilized to calculate the time-history vibration data of the structure in air. The Stochastic Subspace Identification (SSI) method is used to identify the natural frequencies and vibration modes [11]. The calculation process is shown in Fig. 9.

The analysis time length is 1.2 s, and the step time is 0.001 s. In the simulation, an excitation point should be picked to provide vibration motivation on the structure. The time-history displacement in $z$-direction of the excitation point is set as follows:

$$z_{\mathrm{excitation}}(t) = \sum_{i=1}^{100} 0.75^{(i-1)} \sin[2i\pi(t-0.2)] \times 10^{-8}$$
$$t \in [0.2, 1.2]$$

**Table 2** Frequencies of the structures in vacuum environment (Hz)

| | 1st | 2nd | 3rd | 4th | 5th |
|---|---|---|---|---|---|
| Full-area membrane | 32.32 | 44.53 | 56.95 | 59.56 | 64.66 |
| Grid membrane | 32.84 | 45.17 | 55.21 | 58.92 | 64.86 |
| Relative deviation | 1.61% | 1.44% | 3.06% | 1.07% | 0.31% |

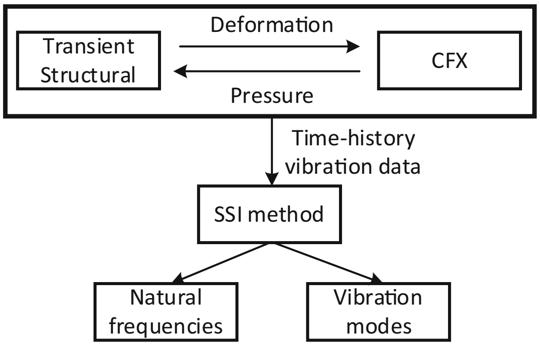


**Fig. 9** FSI calculation and modal identification process

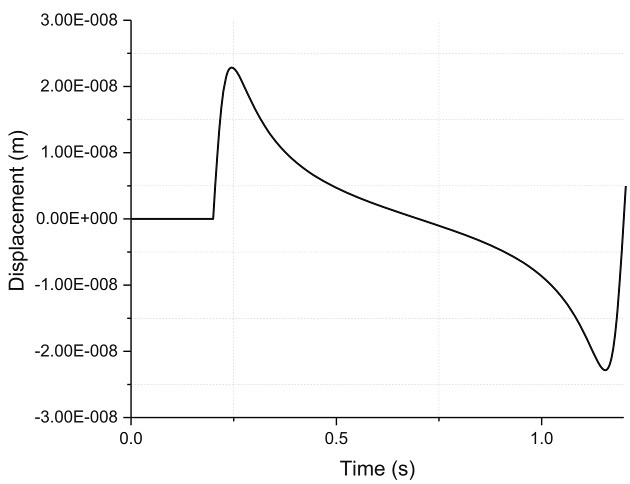


**Fig. 10** The time-history displacement curve of the excitation point

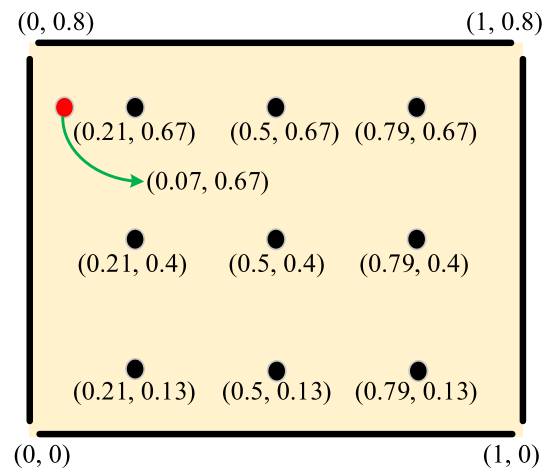


**Fig. 11** The excitation point and observation points of the full-area membrane

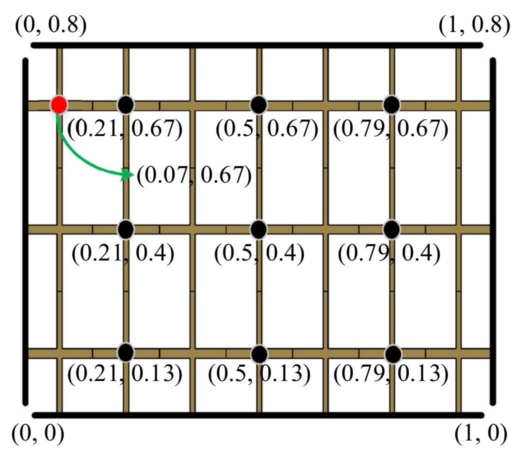


**Fig. 12** The excitation point and observation points of the grid membrane

Therefore, this excitation contains the vibration frequencies from 1 to 100 Hz. The total amplitude is less than $2.5 \times 10^{-8}$ mm, so this vibration is within the scope of the small deformation theory. During the simulation period $t \in [0, 0.2)$, the pre-tension is loaded onto the structure. The time-history displacement curve of the excitation point is shown in Fig. 10.

Node 1 with coordinate (0.07 m, 0.67 m) of the original full-area membrane is chosen as the excitation point (red dot), and the observation points (black dots) are picked as shown in Fig. 11. Node 2 with coordinate (0.07 m, 0.67 m) of the alternative grid membrane is chosen as the excitation point (red dot), and the observation points (black dots) are picked as shown in Fig. 12.

The time-history data from 0.2 to 1.2 s is selected to identify the vibration modal of the structures. Since the nonlinearity of this FSI calculation process is strong, the identified modals are not quite standard, and the fifth modal of the full-area is missing. However, the identified modals are basically valid. Therefore, only the first four modals are considered in the following analysis. The identified modes are shown in Figs. 13 and 14, and the related frequencies are shown in Table 3.

According to Table 3, air has an obvious influence on the full-area membrane: the frequencies in air are far different

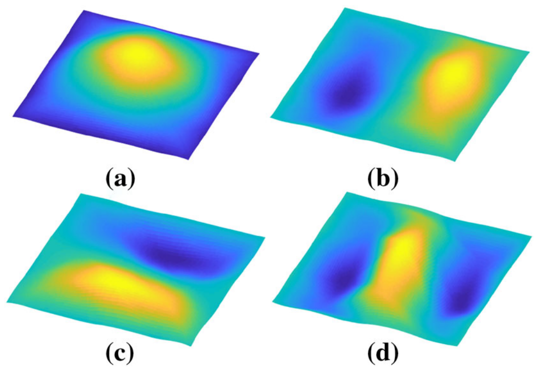

**Fig. 13** Identified modes of full-area membrane in air. **a** 1st mode; **b** 2nd mode; **c** 3rd mode; **d** 4th mode

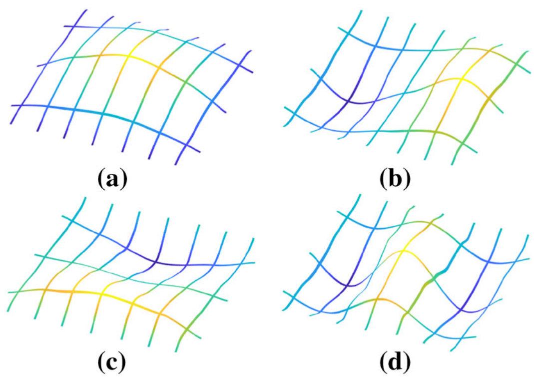

**Fig. 14** Identified modes of grid membrane in air. **a** 1st mode; **b** 2nd mode; **c** 3rd mode; **d** 4th mode

**Table 3** Frequencies of the structures in vacuum and air

| | Full-area membrane | | Grid membrane | |
|---|---|---|---|---|
| | In vacuum (Hz) | In air (Hz) | In vacuum (Hz) | In air (Hz) |
| 1st | 32.32 | 15.19 | 32.84 | 32.42 |
| 2nd | 44.53 | 24.82 | 45.17 | 44.69 |
| 3rd | 56.95 | 33.46 | 55.21 | 54.07 |
| 4th | 59.56 | 37.17 | 58.92 | 58.08 |

from the frequencies in vacuum; however, the frequencies in air and vacuum of the grid membrane are basically same, and the relative deviations are about 2%. Therefore, the grid membrane can be applied as the alternative structure when conducting a ground structure experiment.

## 4 Conclusion

To eliminate the air effect on the membrane in a ground vibration experiment, a grid membrane is explored as the alternative structure. Based on the small deformation theory, a modal equivalent method of a full-area membrane and a grid membrane has been established to make the vibration modal of the grid membrane consistent with the full-area membrane. To verify this equivalent method, an FE code is used to calculate the modals of the two structures in vacuum environment. The modal of the alternative grid membrane is basically identical to the original full-area membrane. Moreover, an FSI simulation is conducted, and the result indicates the air effect on the alternative grid membrane is quite small compared with the original full-area membrane. Consequently, this grid membrane can be applied as the alternative structure when conducting a ground structure experiment. In addition, the proposed modal equivalent method is valid when considering small deformation.

**Funding** This work was supported by the National Natural Science Foundation of China (Nos. 51778362, 51478264, 51608320), the Advanced Research Projects of China Manned Space Project (Granted No. 040203), and the National Postdoctoral Program for Innovative Talents of China (Grant. BX201600104).

## Compliance with ethical standards

**Conflict of interest** The authors declare that they have no conflict of interest.

## Appendix A

To simplify Eqs. (12) and (13), firstly, the integration term can be transformed as follows:

$$\sum_{i=1}^{n_{x\_2}} \int_{y_{i\_2\_1}}^{y_{i\_2\_2}} \sin^2\left(\frac{n\pi y}{b_2}\right)\mathrm{d}y = \frac{1}{2}\sum_{i=1}^{n_{x\_2}} \int_{y_{i\_2\_1}}^{y_{i\_2\_2}} \left[1-\cos\left(\frac{2n\pi y}{b_2}\right)\right]\mathrm{d}y$$

$$= \frac{n_{x\_2}}{2} d_{x\_2} - \frac{b_2}{4n\pi}\sum_{i=1}^{n_{x\_2}} \left[\begin{array}{l} \sin\left(\frac{2in\pi}{n_{x\_2}} - \frac{n\pi}{n_{x\_2}} + n\pi\frac{d_{x\_2}}{b_2}\right) \\ -\sin\left(\frac{2in\pi}{n_{x\_2}} - \frac{n\pi}{n_{x\_2}} - n\pi\frac{d_{x\_2}}{b_2}\right) \end{array}\right]$$

$$= \frac{n_{x\_2}}{2} d_{x\_2} - \frac{b_2}{4n\pi}\sin\left(n\pi\frac{d_{x\_2}}{b_2}\right)\sum_{i=1}^{n_{x\_2}} \left[\sin\left(\frac{2in\pi}{n_{x\_2}} - \frac{n\pi}{n_{x\_2}}\right)\right]$$

$$= \frac{n_{x\_2}}{2} d_{x\_2} - \frac{b_2}{4n\pi}\sin\left(n\pi\frac{d_{x\_2}}{b_2}\right) \times \left[\begin{array}{l} \cos\left(\frac{n\pi}{n_{x\_2}}\right)\sum_{i=1}^{n_{x\_2}}\sin\left(\frac{2in\pi}{n_{x\_2}}\right) \\ -\sin\left(\frac{n\pi}{n_{x\_2}}\right)\sum_{i=1}^{n_{x\_2}}\cos\left(\frac{2in\pi}{n_{x\_2}}\right) \end{array}\right]$$

when $n_{x\_2}$ is odd, we can get that

$$\sum_{i=1}^{n_{x\_2}} \sin\frac{2in\pi}{n_{x\_2}} = \sum_{i=1}^{\frac{n_{x\_2}-1}{2}} \left[\sin\frac{2in\pi}{n_{x\_2}} + \sin\frac{2\left(n_{x\_2}-i\right)n\pi}{n_{x\_2}}\right] + \sin\frac{2n_{x\_2}n\pi}{n_{x\_2}} = 0$$

when $n_{x\_2}$ is even, we can get that

$$\sum_{i=1}^{n_{x\_2}} \sin\frac{2in\pi}{n_{x\_2}} = \sum_{i=1}^{\frac{n_{x\_2}}{2}-1}\left[\sin\frac{2in\pi}{n_{x\_2}} + \sin\frac{2\left(n_{x\_2}-i\right)n\pi}{n_{x\_2}}\right] + \sin\frac{n_{x\_2}n\pi}{n_{x\_2}} + \sin\frac{2n_{x\_2}n\pi}{n_{x\_2}} = 0$$

Therefore

$$\sum_{i=1}^{n_{x\_2}} \sin\frac{2in\pi}{n_{x\_2}} = 0$$

Meanwhile,

$$\sin\frac{n\pi}{n_{x\_2}}\sum_{i=1}^{n_{x\_2}} \cos\frac{2in\pi}{n_{x\_2}} = \frac{1}{2}\left[\sum_{i=1}^{n_{x\_2}} \sin\frac{n\pi}{n_{x\_2}}(2i+1) - \sum_{i=1}^{n_{x\_2}} \sin\frac{n\pi}{n_{x\_2}}(2i-1)\right] = \frac{1}{2}\left[\sin\frac{n\pi}{n_{x\_2}} - \sin\frac{n\pi}{n_{x\_2}}\right] = 0$$

Therefore, when $\sin\frac{n\pi}{n_{x\_2}} \neq 0$, meaning $\frac{n}{n_{x\_2}} \notin \mathbf{Z}$, we can get that

$$\sum_{i=1}^{n_{x\_2}} \cos\frac{2in\pi}{n_{x\_2}} = 0$$

Consequently, when $\frac{n}{n_{x\_2}} \notin \mathbf{Z}$,

$$\sum_{i=1}^{n_{x\_2}} \int_{y_{i\_2\_1}}^{y_{i\_2\_2}} \sin^2\left(\frac{n\pi y}{b_2}\right)\mathrm{d}y = \frac{n_{x\_2}}{2} d_{x\_2}$$

Similarly, when $\frac{m}{n_{y\_2}} \notin \mathbf{Z}$, we can get that

$$\sum_{i=1}^{n_{y\_2}} \int_{x_{i\_2\_1}}^{x_{i\_2\_2}} \sin^2\left(\frac{m\pi x}{a_2}\right)\mathrm{d}x = \frac{n_{y\_2}}{2} d_{y\_2}$$

Consequently, when $\frac{n}{n_{x\_2}} \notin \mathbf{Z}$, $\frac{m}{n_{y\_2}} \notin \mathbf{Z}$, we can get that

$$\begin{aligned} A_{mn\_2} &= \oiint_{S_{x\_2}} Z_{mn\_2}^2 \mathrm{d}S + \oiint_{S_{y\_2}} Z_{mn\_2}^2 \mathrm{d}S \\ &= \sum_{i=1}^{n_{x\_2}}\left[\int_0^{a_2} \sin^2\left(\frac{m\pi x}{a_2}\right)\mathrm{d}x \int_{y_{i\_2\_1}}^{y_{i\_2\_2}} \sin^2\left(\frac{n\pi y}{b_2}\right)\mathrm{d}y\right] \\ &\quad + \sum_{i=1}^{n_{y\_2}}\left[\int_{x_{i\_2\_1}}^{x_{i\_2\_2}} \sin^2\left(\frac{m\pi x}{a_2}\right)\mathrm{d}x \int_0^{b_2} \sin^2\left(\frac{n\pi y}{b_2}\right)\mathrm{d}y\right] \\ &= \frac{a_2 n_{x\_2}}{4} d_{x\_2} + \frac{b_2 n_{y\_2}}{4} d_{y\_2} \end{aligned}$$

Meanwhile, the frequency expression can be simplified as follows:

$$\begin{aligned} \omega_{mn\_2}^2 &= -\frac{N_{x0\_2}}{\rho_2 h_2 A_{mn\_2}} \oiint_{S_{x\_2}} \frac{\partial^2 Z_{mn}}{\partial x^2} Z_{mn} \mathrm{d}S - \frac{N_{y0\_2}}{\rho_2 h_2 A_{mn\_2}} \oiint_{S_{y\_2}} \frac{\partial^2 Z_{mn}}{\partial y^2} Z_{mn} \mathrm{d}S \\ &= \frac{1}{\rho_2 h_2 A_{mn\_2}}\left[\frac{a_2 N_{x0\_2}}{2}\left(\frac{m\pi}{a_2}\right)^2 \sum_{i=1}^{n_{x\_2}} \int_{y_{i\_2\_1}}^{y_{i\_2\_2}} \sin^2\left(\frac{n\pi y}{b_2}\right)\mathrm{d}y + \frac{b_2 N_{y0\_2}}{2}\left(\frac{n\pi}{b_2}\right)^2 \sum_{i=1}^{n_{y\_2}} \int_{x_{i\_2\_1}}^{x_{i\_2\_2}} \sin^2\left(\frac{m\pi x}{a_2}\right)\mathrm{d}x\right] \\ &= \frac{1}{\rho_2 h_2 A_{mn\_2}}\left[N_{x0\_2}\left(\frac{m\pi}{a_2}\right)^2 \frac{a_2 n_{x\_2}}{4} d_{x\_2} + N_{y0\_2}\left(\frac{n\pi}{b_2}\right)^2 \frac{b_2 n_{y\_2}}{4} d_{y\_2}\right] \end{aligned}$$

## References


1. Li Y et al (2011) Added-mass estimation of flat membranes vibrating in still air. J Wind Eng Ind Aerodyn 99(8):815–824
2. Chen YF et al (2013) Analysis and Test of the Inflatable Tubes of ETFE Foils. Appl Mech Materials 351–352:892–896
3. Hu Y et al (2017) Modal behaviors and influencing factors analysis of inflated membrane structures. Eng Struct 132:413–427
4. Zhou Y et al (2018) Study on added mass of a circular curved membrane vibrating in still air. Thin Walled Struct 127:200–209
5. Liu F, Jin D, Wen H (2017) Equivalent dynamic model for hoop truss structure composed of planar repeating elements. AIAA J 55(3):1058–1063
6. Xu R et al (2015) Nonlinear vibration analysis of membrane SAR antenna structure adopting a vector form intrinsic finite element. J Mech 31(3):269–277
7. Apedo KL et al (2010) Nonlinear finite element analysis of inflatable beams made from orthotropic woven fabric. Int J Solids Struct 47(16):2017–2033
8. Nguyen QT, Thomas JC, Van AL (2015) Inflation and bending of an orthotropic inflatable beam. Thin Walled Struct 88:129–144
9. Lecieux Y, Bouzidi R (2010) Experimental analysis on membrane wrinkling under biaxial load—comparison with bifurcation analysis. Int J Solids Struct 47(18):2459–2475
10. Mianroodi JR et al (2011) Nonlinear membrane model for large amplitude vibration of single layer graphene sheets. Nanotechnology 22(30):305703
11. Peeters B, Roeck GD (1999) Reference-based stochastic subspace identification for output-only modal analysis. Mech Syst Signal Process 13(6):855–878